Paramagnetism and relaxation dynamics in melanin biomaterials

THE JOURNAL OF PHYSICAL CHEMISTRY B

B: Biophysics; Physical Chemistry of Biological Systems and Biomolecules

Paramagnetism and Relaxation Dynamics in Melanin Biomaterials

Maher Al Khatib, Jessica Costa, Maria Camilla Baratto, Riccardo Basosi, and Rebecca Pogni

J. Phys. Chem. B, **Just Accepted Manuscript** • DOI: 10.1021/acs.jpcb.9b11785 • Publication Date (Web): 27 Feb 2020

Paramagnetism and Relaxation Dynamics in Melanin Biomaterials

*Maher Al Khatib, Jessica Costa, Maria Camilla Baratto, Riccardo Basosi and Rebecca Pogni**

Department of Biotechnology, Chemistry and Pharmacy, Via A. Moro 2, 53100 Siena (Italy)

ABSTRACT

The spectroscopical characterization of melanins is a prior requirement for the efficient tailoring of their radical scavenging, UV-Vis radiation absorption, metal chelation and natural pigment properties. The Electron Paramagnetic Resonance (EPR), exploiting the common persistent paramagnetism of melanins, represents the elective standard for the structural and dynamical characterization of their constituting radical species. As much as melanins are mainly investigated using X-band (9.5 GHz) CW- EPR, an integration with an alternative application of Q-band (34 GHz) in CW and pulse EPR for the discrimination of melanin pigments of different composition is here presented. The longitudinal relaxation times measured highlight faster relaxation rates for cysteinyldopa melanin, compared to those of the most common dopa melanin pigment, suggesting pulse EPR spin-lattice relaxation time measurements as a complementary tool for characterization of pigments of interest for biomimetic materials engineering.

INTRODUCTION

Bioinspired materials are designed to mimic the biological, chemical and physical properties of extraordinary materials present in nature. The variety with which nature expresses itself can be exploited for the realization of biocompatible materials to support the needs and challenges of a green-economy logic. In this context melanin pigments have attracted an increasing degree of attention due to their potential applications in the realization of optoelectronical and biomedical devices.[1-11] Melanins are ubiquitous pigments present in nature, which exhibit peculiar adhesive properties, a wide UV-vis light absorption spectrum, capability of acting as mixed ionic-electronic conductors and marked metal ions chelator and free radical scavenging activities. [12–24]

Due to the lower immunoresponse in in-vitro tests, melanins have been proposed for electro-medical devices coatings.[8] Furthermore, melanins are commonly known for their characteristic black to reddish color span, and the exploitation of their structural and geometrical spatial organization has been proven successfully for the realization of structural colors.[25–32] In fact, melanin's highly heterogeneous structural and geometrical features at the nano and micro scale contribute to most of their characteristic physico-chemical properties, such as the increasing absorption trend toward the blue region of the UV-Vis spectrum.[33] This high structural heterogeneity poses a challenge for the melanin characterization necessary for a controlled design and engineering of functional melanin materials.[34,35] At the state of the art, the most successful characterization of melanin pigments is being achieved using continuous wave (CW) electron paramagnetic resonance spectroscopy (EPR), which exploits the characteristic persistence of free radical species common to all melanins to extract structural and dynamical information (e.g. free radical composition).[36–42] EPR investigation, together with the support of computational studies, helped to identify 5,6-dihydroxyindole (DHI) and 5,6-dihydroxyindole-2-carboxylic acid (DHICA) as the main constituents of the most common melanin form found in

nature, eumelanin (also known as dopa-melanin), while cysteinyldopa derived units have been found as characteristic components of pheomelanin (also known as cysteinyldopa melanin).[5,13,43–46] Electrochemical fingerprinting has been used to suggest that natural eumelanin pigments contain porphyrin-like proto-molecules composed of DHI/DHICA tetramers, while recent computational investigations describe melanins as composed of a mixture of low molecular weight oligomers.[43,47]

In this paper, the paramagnetic properties of enzymatically produced dopa melanin and cysteinyldopa melanin, have been probed by the use of Q-band (34 GHz) pulse EPR and Q- and X-band (9 GHz) CW Multifrequency EPR. The use of selective microwave pulses at Q-band frequencies was employed to measure the longitudinal relaxation times of these two different melanin pigments, providing the evidence that faster relaxation dynamics are present in cysteinyldopa melanin and that the EPR pulse technique can represents an useful and complementary tool to discriminate between the two different pigments.

EXPERIMENTAL SECTION

Sample preparation. Two different samples were prepared by the oxidative activity of *Trametes versicolor* (*T.v.*) laccase (12.9 U mg^{-1}) in 100 mM phosphate buffer (pH=7.1) and dopa (6.57 mg/mL) (1:1000 Lac:dopa molar ratio) for dopa melanin synthesis and 1:2 dopa:cysteine molar ratio in acetate buffer 100 mM (pH=4.5) for cysteinyldopa.[13] The formation of a markedly insoluble black and reddish pigments respectively were obtained. The synthesis was performed at room temperature at air under stirring for 16 h. The samples were dried under nitrogen flux and collected as dry powders. The powders were inserted within cylindrical Suprasil capillaries for EPR Q-band measurements (WG-222T-RB, Cortecnet Europe, France) with ID x OD equal

to 1.1x1.6 mm. The same samples were used for CW X- and Q-band and pulse Q-band EPR measurements. Possible samples hydration cannot be ruled out.

EPR experimental setup. EPR spectra were measured with a Bruker ELEXSYS E580 Super Q-FT spectrometer, equipped with ER 5107D2 probehead, CF935 continuous-flow helium cryostat (Oxford Instruments), and ITC 502 temperature controller (Oxford Instruments) for CW and pulse Q-band EPR measurements. CW X-band spectra and spin quantitation measurements were performed using a Bruker ER 049X microwave bridge with 4122SHQE/0208 cavity. The spin quantitation was carried out against an internal reference (Bruker) of irradiated solid alanine (3mm length, 5mm diameter) sealed under N_2 atmosphere, and containing a total of $2.05 \cdot 10^{-7}$ ±10% spins, using the SpinCounting program provided in the Xepr software (Bruker).

Q-band pulse experiments. The Echo Detected Field Sweep spectra of the two melanin samples were acquired with a $\pi/2$-τ-π echo sequence ($\pi/2$=42 ns and π=84 ns). A Picket Fence Saturation Recovery sequence (PFSR) (**Scheme 1**) was used for the measurement of longitudinal relaxation times.

Scheme 1. Picket Fence Saturation Recovery sequence. Saturation and detection microwave pulses were used to measure longitudinal relaxation times.

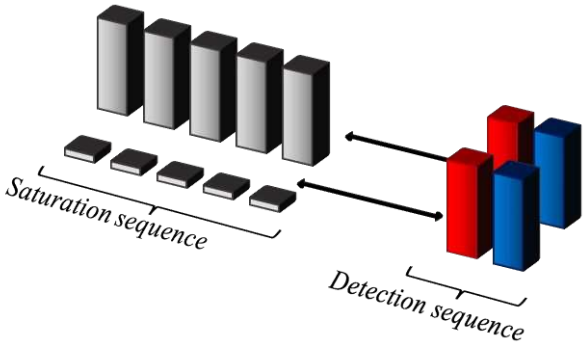

The region of the EPR spectra corresponding to the maximum of absorption was irradiated with a train of 29 saturating rectangular π/2 microwave pulses (higher grey pulses in **Scheme 1**), and the value of the residual magnetization was sampled with a rectangular pulses π/2-τ-π echo detection sequence (red and blue pulses respectively). In order to assess the effective saturation recovery, the equilibrium value of the magnetization was acquired running a PFSR experiment where the saturating pulses were turned off (lower grey pulses).

RESULTS AND DISCUSSION

The CW-EPR technique is greatly employed for the characterization of melanin free radical species. However, the g-value, intensity and lineshape of the spectrum are the sole observables obtained from a CW-EPR spectrum as no hyperfine structure is observed. In the context of relaxation time measurements, melanin pigments characterization was carried out in the pioneering work by Sarna and Hyde on 1978, while pulse EPR has been long underexploited for melanin radicals' characterization, with the exception of the landmark X-band pulse EPR paper of Okazaki et al. dating back to 1985.[48,49]

In **Figure 1a** and **1b**, the EPR spectra recorded at increasing microwave power (max power value, M_0=144.5 mW), for the dopa melanin (g_{iso}=2.0036±0.0002, Figure 1a) and cysteinyldopa melanin (g_{iso}=2.0050±0.0002, Figure 1b) samples are shown. The dopa melanin free radical signal (peak to peak signal amplitude, ΔB_{pp}= 0.5±0.1 mT, at microwave power M=1.46 mW) is commonly interpreted as originating from the concomitant presence of carbon centered

(g~2.0032) and semiquinone (g~2.0045) free radical species, whose respective contributions to the EPR signals are function of the hydration level and pH of the sample.[50] The free radical signal recorded in cysteinyldopa melanins on the other hand, with its higher g value (g~2.0050) and broader lineshape (central line peak to peak signal amplitude, ΔB_{pp}=3.2±0.1 mT, at microwave power M=1.46 mW), is attributed to the presence of semiquinonimine free radical species.[51,52]

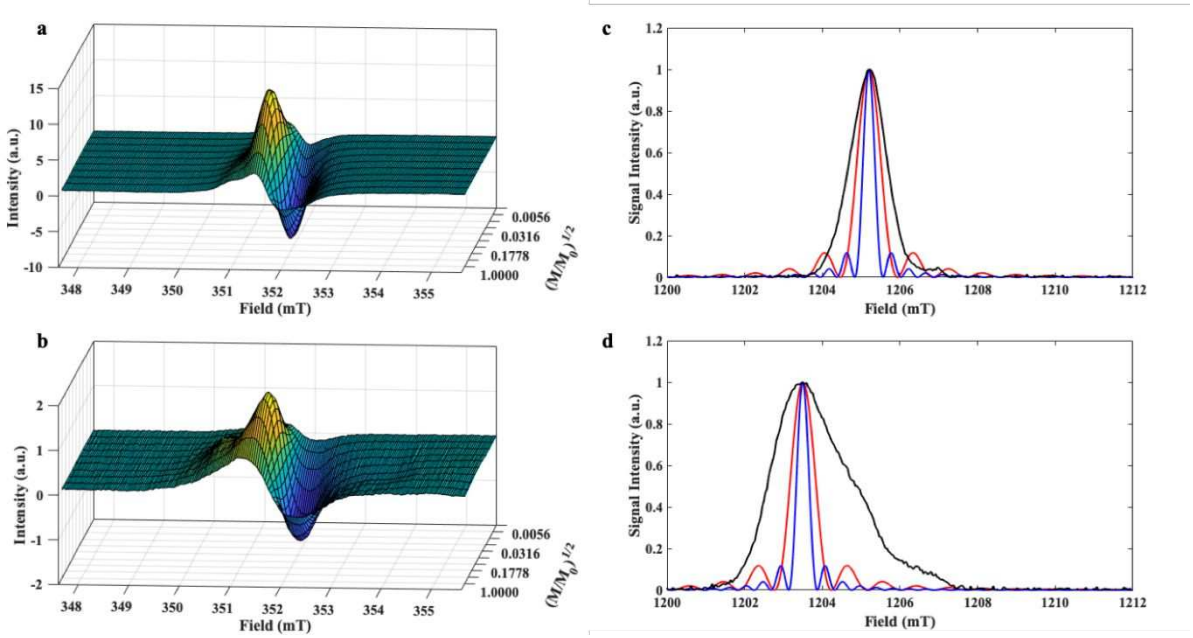

Figure 1. Left panel - (a) X-band (ν=9.871 GHz) room temperature power saturation curves of dopa melanin. (b) X-band (ν=9.877 GHz) room temperature power saturation curves of the cysteinyldopa melanin. Right panel – (c) Echo Detected Field Sweep (EDFS) spectra recorded at Q-band for dopa melanin and (d) cysteinyldopa melanin samples. The red and blue curves in (c) and (d) represent the spectral lineshape of the rectangular π/2 and π pulses respectively used to generate the electron spin echo for the EDFS spectra acquisition.

The intensity increase of the X-band EPR signal for dopa and cysteinyldopa samples reaches a maximum and then decreases with higher microwave power levels (**Figure S1**). The same trend is also evident in the EPR spectra recorded at Q-band (**Figure S2**). This progress of the EPR lines suggests a homogeneous line broadening with the absence of the so-called spin-islands with a free radical spin density equal to ~$5.84 \cdot 10^{13}$ spins/mm^3 for dopa melanin and ~$2.20 \cdot 10^{13}$ spins/mm^3 for the cysteinyldopa melanin respectively.[41]

To investigate the possible use of relaxation time as a novel observable to differentiate melanin samples, pulse Q-band EPR (34 GHz) was employed for longitudinal relaxation time (T_1) determination. The solid state Q-band EPR experiments will be of great help as at this frequency the g values and the anisotropies of the different radical species are better solved. Room temperature Q-band Echo Detected Field Sweep (EDFS) spectra of the samples were first recorded, in order to set the region of spectra to be selected for further investigations (**black lines in Figure 1c and 1d**). Rectangular microwave pulses of $\pi/2$=42 ns and π=84 ns (full-width-half-height linewidth of ~29 MHz and 14 MHz respectively - **red and blue lines in Figure 1c and 1d**) were then optimized for the relaxation study sequences further used. The spectral coverage of the $\pi/2$ and π microwave pulses was centered in correspondence of the maximum of the absorption spectra of the dopa melanin and cysteinyldopa melanin. The room temperature phase memory time (T_M) of the two pigments was measured in place of the transverse relaxation time T_2 in order to take into account the effect of instantaneous diffusion. The latter can contribute to the transverse relaxation process at the relatively low concentrations of paramagnetic centers in the samples (lower than 10^{15} spins/mm^3).[53] The phase memory time T_M was extracted from the echo decay curves (**Figure S3**) using a monoexponential model, $y = A \cdot exp(-t/T_M) + c$, yielding T_M~262 ns for the dopa melanin and T_M~228 ns for cysteinyldopa melanin samples.

Differences in relaxation times were emphasized when the longitudinal relaxation time (T_1) was measured. T_1 measurements were performed with Picket Fence Saturation Recovery (PFSR) experiments, to minimize the effect of spectral diffusion.[54] The saturation recovery measurements were performed in the temperature range 20-110 K (Figure 2). The longitudinal relaxation times were extracted from the saturation curves, using the biexponential model $y = A_f \cdot exp(-t/T_{1f}) + A_s \cdot exp(-t/T_{1s}) + c$, which considered the presence of two concurring mechanisms contributing to the longitudinal relaxation process, described by different T_1 parameters, namely T_{1f} and T_{1s}. The T_{1f} component, is representative of the spectral diffusion effects, while the T_{1s} component of the actual longitudinal relaxation process.

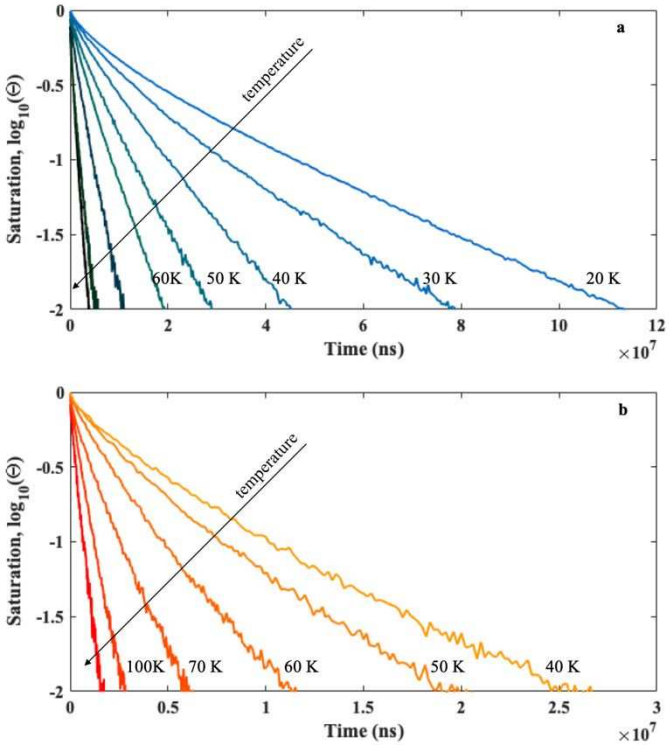

Figure 2. Q-band PFSR curves acquired at variable temperature for the (a) dopa melanin and (b) cysteinyldopa melanin samples. The $\log_{10}(\Theta)$ represents the saturation recovery process of the

macroscopic magnetization in the two samples. The level of saturation percentage is indicated as Θ. The arrow indicates the increasing temperature.

The saturation curves reported in Figure 2a and 2b, show how the saturated magnetization of the melanin pigments is recovered with time from the starting point of total saturation condition, i.e. Θ=1, towards the point of saturation recovery, i.e. Θ→0.

Together with the data reported in **Table 1**, Figure 2 depicts the longitudinal relaxation process for the two biomaterials investigated. Faster spin-lattice relaxations were measured for the cysteinyldopa melanin over the entire temperature range. The smaller cysteinyldopa T_{1f} and T_{1s} values can be attributed to the different nature of its radical species. At 40 K (the lowest common temperature investigated for the two pigments), the composed semiquinonimine radical signal of the cysteinyldopa melanin recovered the 99% of the equilibrium magnetization level in approximately $2.5 \cdot 10^{-2}$ s. The same recovery of the equilibrium magnetization level was reached after approximately $4.5 \cdot 10^{-2}$ s in the case of dopa melanin.

Table 1. Longitudinal relaxation times. The columns report the T_{1f} and T_{1s} values evaluated for the dopa melanin and cysteinyldopa melanin samples

	Dopa melanin		**Cysteinyldopa melanin**	
T(K)	**T_{1f} (μs)[a)]**	**T_{1s} (μs) [a)]**	**T_{1f} (μs) [a)]**	**T_{1s} (μs) [a)]**
20	1.15E+04	6.79E+04	-	-
30	1.06E+04	4.90E+04	-	-
40	5.42E+03	2.60E+04	6.07E+03	2.09E+04
50	3.93E+03	1.69E+04	4.91E+03	1.69E+04
60	2.95E+03	1.12E+04	2.74E+03	8.31E+03

70	2.09E+03	6.73E+03	1.94E+03	5.68E+03
100	1.53E+03	4.79E+03	7.16E+02	1.90E+03
110	9.70E+02	2.66E+03	4.14E+02	1.09E+03

[a)] The error on the reported T_{1f} and T_{1s} values obtained with the biexponential decay model, was estimated to ±3 μs

The presence of cysteinyldopa melanin is commonly detected by higher values of the electronic g-factor and by the more complex lineshape resolved by CW EPR. Due to the relatively high difference in terms of spin-lattice relaxation times for the two compounds at higher temperature (approaching 60% at 100 K), Q-band PFSR measurements can be proposed as a complementary tool to classic multifrequency CW EPR for the assessment of the nature of new melanin pigments of unknown composition, and as an insightful instrument in melanin radical characterization.

Room temperature PFSR experiments were also performed to assess the measurements of relaxation times as discriminant feature under common melanins functional conditions (T = 298K) (**Figure 3**).

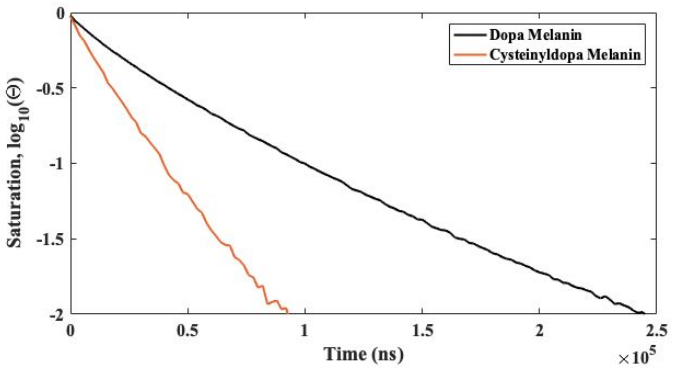

Figure 3 Q-band room temperature (298 K) PFSR curves recorded for dopa melanin (black) and cysteinyldopa melanin (orange). Dopa melanin ν=33.843 GHz; cysteinyldopa melanin ν=33.733 GHz.

Figure 3 and **Table 2** show that cysteinyldopa faster longitudinal relaxation dynamics point out the feasibility of running T_1 measurement as discriminant feature for melanin characterization even when EPR room temperature experiments are considered.

Table 2. Room temperature $\mathbf{T_{1f}}$ and $\mathbf{T_{1s}}$ values for the dopa and cysteinyldopa melanins.

Sample	$\mathbf{T_{1f}}$ **(μs)**[a)]	$\mathbf{T_{1s}}$ **(μs)**[a)]
Dopa melanin	61	216
Cysteinyldopa melanin	23	58

[a)] The error on the reported T_{1f} and T_{1s} values obtained with the biexponential decay model was estimated to ±3μs

Moreover, the T_1 values measured for the dopa melanin produced by laccase (melanin pigments are commonly produced either using tyrosinase or by chemical oxidation of the substrate –tyrosine or dopa), could be compared with those obtained by Okazaki et all., where values of T_1~4 ms were recorded for dopa melanins (77 K), indicating consistency in T_1 values for dopa melanin pigments of different origin.

CONCLUSIONS

This preliminary combined pulse and Multifrequency EPR investigation on representative melanins contributes to fill a gap in the rich literature of EPR characterization of melanin pigments.[48] The characterization of the relaxation properties will certainly introduce a new tool to identify and gain information on the pigments, whose structures heterogeneity in solid state

are still object of intensive research, and whose understanding would open up new doors in biopigment material design.[17]

The same pulse EPR experiments could be extended to other conductive polymers like polyanilines, where the distribution of relaxation times values could be linked to the different polymer chain size, but also to more complex system like the melanin-polyaniline conductive biopolymers of technological interest.[55–58]

AUTHOR INFORMATION

Corresponding Author

* E-mail: rebecca.pogni@unisi.it, Department of Biotechnology, Chemistry and Pharmacy, Via A. Moro 2, 53100 Siena (Italy).

ASSOCIATED CONTENT

Supporting Information

Figure S1. X-band CW saturation curves for the dopa melanin and cysteinyldopa melanin.

Figure S2. Q-band CW saturation curves for the dopa melanin and cysteinyldopa melanin.

Figure S3. Phase memory time measurements for dopa melanin and cysteinyldopa melanin.

ACKNOWLEDGMENTS

CSGI (Consorzio per lo Sviluppo dei Sistemi a Grande Interfase), Florence, Italy and MIUR for the Dipartimento di Eccellenza 2018-2022 grant are gratefully acknowledged.

REFERENCES

(1) Wang, Y.; Wang, X.; Li, T.; Ma, P.; Zhang, S.; Du, M.; Dong, W.; Xie, Y.; Chen, M. Effects of Melanin on Optical Behavior of Polymer: From Natural Pigment to Materials Applications. *ACS Appl. Mater. Interfaces* **2018**, *10*, 13100–13106.

(2) Nune, M.; Manchineella, S.; Govindaraju, T.; Narayan, K. S. Melanin Incorporated Electroactive and Antioxidant Silk Fi Broin Nano Fi Brous Sca Ff Olds for Nerve Tissue Engineering. *Mater. Sci. Eng. C* **2019**, *94*, 17–25.

(3) D'Ischia, M. Melanin-Based Functional Materials. *Int. J. Mol. Sci.* **2018**, *19*, 1–4.

(4) Kim, Y. J. o.; Wu, W.; Chun, S. E.; Whitacre, J. F.; Bettinger, C. J. Catechol-Mediated Reversible Binding of Multivalent Cations in Eumelanin Half-Cells. *Adv. Mater.* **2014**, *26*, 6572–6579.

(5) D'Ischia, M.; Napolitano, A.; Ball, V.; Chen, C. T.; Buehler, M. J. Polydopamine and Eumelanin: From Structure-Property Relationships to a Unified Tailoring Strategy. *Acc. Chem. Res.* **2014**, *47*, 3541-3550.

(6) Migliaccio, L.; Manini, P.; Altamura, D.; Giannini, C.; Tassini, P.; Maglione, M. G.; Minarini, C.; Pezzella, A. Evidence of Unprecedented High Electronic Conductivity in Mammalian Pigment Based Eumelanin Thin Films after Thermal Annealing in Vacuum. *Front. Chem.* **2019**, *7*, 1–8.

(7) Di Capua, R.; Gargiulo, V.; Alfè, M.; De Luca, G. M.; Skála, T.; Mali, G.; Pezzella, A. Eumelanin Graphene-like Integration: The Impact on Physical Properties and Electrical Conductivity. *Front. Chem.* **2019**, *7*, 1–12.

(8) Eom, T.; Woo, K.; Cho, W.; Heo, J. E.; Jang, D.; Shin, J. I.; Martin, D. C.; Wie, J. J.; Shim, B. S. Nanoarchitecturing of Natural Melanin Nanospheres by Layer-by-Layer Assembly: Macroscale Anti-Inflammatory Conductive Coatings with Optoelectronic Tunability. *Biomacromolecules* **2017**, *18*, 1908–1917.

(9) D'Ischia, M.; Napolitano, A.; Pezzella, A.; Meredith, P.; Sarna, T. Chemical and Structural Diversity in Eumelanins: Unexplored Bio-Optoelectronic Materials. *Angew. Chemie - Int. Ed.* **2009**, *48*, 3914–3921.

(10) Kumar, P.; Di Mauro, E.; Zhang, S.; Pezzella, A.; Soavi, F.; Santato, C.; Cicoira, F. Melanin-Based Flexible Supercapacitors. *J. Mater. Chem. C* **2016**, *4*, 9516–9525.

(11) Goerlitzer, E. S. A.; Klupp Taylor, R. N.; Vogel, N. Bioinspired Photonic Pigments from Colloidal Self-Assembly. *Adv. Mater.* **2018**, *30*, 1–15.

(12) D'Ischia, M.; Wakamatsu, K.; Cicoira, F.; Di Mauro, E.; Garcia-Borron, J. C.; Commo, S.; Galván, I.; Ghanem, G.; Kenzo, K.; Meredith, P.; et al. Melanins and Melanogenesis: From Pigment Cells to Human Health and Technological . *Pigment Cell Melanoma Res.*

2015, *28*, 520–544.

(13) D'Ischia, M.; Wakamatsu, K.; Napolitano, A.; Briganti, S.; Garcia-Borron, J. C.; Kovacs, D.; Meredith, P.; Pezzella, A.; Picardo, M.; Sarna, T.; et al. Melanins and Melanogenesis: Methods, Standards, Protocols. *Pigment Cell Melanoma Res.* **2013**, *26*, 616–633.

(14) Lopiano, L.; Chiesa, M.; Digilio, G.; Giraudo, S.; Bergamasco, B.; Torre, E.; Fasano, M. Q-Band EPR Investigations of Neuromelanin in Control and Parkinson's Disease Patients. *Biochim. Biophys. Acta - Mol. Basis Dis.* **2000**, *1500*, 306–312.

(15) Kautz, R.; Ordinario, D. D.; Tyagi, V.; Patel, P.; Nguyen, T. N.; Gorodetsky, A. A. Cephalopod-Derived Biopolymers for Ionic and Protonic Transistors. *Adv. Mater.* **2018**, *30*, 1–15.

(16) Amdursky, N.; Głowacki, E. D.; Meredith, P. Macroscale Biomolecular Electronics and Ionics. *Adv. Mater.* **2019**, *31*, 1–28.

(17) Jeong, Y. K.; Park, S. H.; Choi, J. W. Mussel-Inspired Coating and Adhesion for Rechargeable Batteries: A Review. *ACS Appl. Mater. Interfaces* **2018**, *10*, 7562–7573.

(18) Solano, F. Melanin and Melanin-Related Polymers as Materials with Biomedical and Biotechnological Applications— Cuttlefish Ink and Mussel Foot Proteins as Inspired Biomolecules. *Int. J. Mol. Sci.* **2017**, *18*, 1–18.

(19) Mostert, A. B.; Powell, B. J.; Pratt, F. L.; Hanson, G. R.; Sarna, T.; Gentle, I. R.; Meredith, P. Role of Semiconductivity and Ion Transport in the Electrical Conduction of Melanin. *Proc. Natl. Acad. Sci.* **2012**, *109*, 8943–8947.

(20) Nawaz, M.; Khan, H. M. S.; Akhtar, N.; Jamshed, T.; Qaiser, R.; Shoukat, H.; Farooq, M. Photodamage and Photoprotection: An In-Vivo Approach Using Non-Invasive Probes. *Photochem. Photobiol.* **2019**, *95*, 1243–1248.

(21) Jakubiak, P.; Lack, F.; Thun, J.; Urtti, A.; Alvarez-Sánchez, R. Influence of Melanin Characteristics on Drug Binding Properties. *Mol. Pharm.* **2019**, *16*, 2549–2556.

(22) Maher, S.; Mahmoud, M.; Rizk, M.; Kalil, H. Synthetic Melanin Nanoparticles as Peroxynitrite Scavengers, Photothermal Anticancer and Heavy Metals Removal Platforms. *Environ. Sci. Pollut. Res.* **2019**, https://doi.org/10.1007/s11356-019-05111-3.

(23) Mostert, A. B.; Rienecker, S. B.; Noble, C.; Hanson, G. R.; Meredith, P. The Photoreactive Free Radical in Eumelanin. *Sci. Adv.* **2018**, *4*, 1–7.

(24) Brunetti, A.; Arciuli, M.; Triggiani, L.; Sallustio, F.; Gallone, A.; Tommasi, R. Do Thermal Treatments Influence the Ultrafast Opto-Thermal Processes of Eumelanin? *Eur. Biophys. J.* **2019**, *48*, 153–160.

(25) Ito, S. Reexamination of the Structure of Eumelanin. *BBA - Gen. Subj.* **1986**, *883*, 155–161.

(26) Godechal, Q.; Ghanem, G. E.; Cook, M. G.; Gallez, B. Electron Paramagnetic Resonance

Spectrometry and Imaging in Melanomas: Comparison between Pigmented and Nonpigmented Human Malignant Melanomas. *Mol. Imaging* **2013**, *12*, 218–223.

(27) Godechal, Q.; Leveque, P.; Marot, L.; Baurain, J. F.; Gallez, B. Optimization of Electron Paramagnetic Resonance Imaging for Visualization of Human Skin Melanoma in Various Stages of Invasion. *Exp. Dermatol.* **2012**, *21*, 341–346.

(28) Xiao, M.; Li, Y.; Allen, M. C.; Deheyn, D. D.; Yue, X.; Zhao, J.; Gianneschi, N. C.; Shawkey, M. D.; Dhinojwala, A. Bio-Inspired Structural Colors Produced via Self-Assembly of Synthetic Melanin Nanoparticles. *ACS Nano* **2015**, *9*, 5454–5460.

(29) Iwasaki, T.; Tamai, Y.; Yamamoto, M.; Taniguchi, T.; Kishikawa, K.; Kohri, M. Melanin Precursor Influence on Structural Colors from Artificial Melanin Particles: PolyDOPA, Polydopamine, and Polynorepinephrine. *Langmuir* **2018**, *34*, 11814–11821.

(30) Capecchi, E.; Piccinino, D.; Bizzarri, B. M.; Avitabile, D.; Pelosi, C.; Colantonio, C.; Calabrò, G.; Saladino, R. Enzyme-Lignin Nanocapsules Are Sustainable Catalysts and Vehicles for the Preparation of Unique Polyvalent Bioinks. *Biomacromolecules* **2019**, *20*, 1975–1988.

(31) Isapour, G.; Lattuada, M. Bioinspired Stimuli-Responsive Color-Changing Systems. *Adv. Mater.* **2018**, *30*, 1–36.

(32) Kolle, M.; Lee, S. Progress and Opportunities in Soft Photonics and Biologically Inspired Optics. *Adv. Mater.* **2018**, *30*, 1–40.

(33) Chen, C. T.; Chuang, C.; Cao, J.; Ball, V.; Ruch, D.; Buehler, M. J. Excitonic Effects from Geometric Order and Disorder Explain Broadband Optical Absorption in Eumelanin. *Nat. Commun.* **2014**, *5*, 1–10.

(34) Roy, S.; Rhim, J.-W. Preparation of Carrageenan-Based Functional Nanocomposite Films Incorporated with Melanin Nanoparticles. *Colloids Surfaces B Biointerfaces* **2019**, *176*, 317–324.

(35) Ribera, J.; Panzarasa, G.; Stobbe, A.; Osypova, A.; Rupper, P.; Klose, D.; Schwarze, F. W. M. R. Scalable Biosynthesis of Melanin by the Basidiomycete Armillaria Cepistipes. *J. Agric. Food Chem.* **2019**, *67*, 132–139.

(36) Paulin, J. V; Batagin-Neto, A.; Graeff, C. F. O. Identification of Common Resonant Lines in the EPR Spectra of Melanins. *J. Phys. Chem. B* **2019**, *123*, 1248–1255.

(37) Desmet, C. M.; Danhier, P.; Acciardo, S.; Levêque, P.; Gallez, B. Towards in Vivo Melanin Radicals Detection in Melanomas by Electron Paramagnetic Resonance (EPR) Spectroscopy: A Proof-of-Concept Study. *Free Radic. Res.* **2019**, *53*, 405–410.

(38) Kaxiras, E.; Tsolakidis, A.; Zonios, G.; Meng, S. Structural Model of Eumelanin. *Phys. Rev. Lett.* **2006**, *97*, 218102.

(39) Ito, S. A Chemist ' s View of Melanogenesis. *Pigment Cells Res* **2003**, *16*, 230–236.

(40) Plonka, P. M. Electron Paramagnetic Resonance as a Unique Tool for Skin and Hair Research. *Exp. Dermatol.* **2009**, *18*, 472–484.

(41) Zdybel, M.; Pilawa, B.; Drewnowska, J. M.; Swiecicka, I. Comparative EPR Studies of Free Radicals in Melanin Synthesized by Bacillus Weihenstephanensis Soil Strains. *Chem. Phys. Lett.* **2017**, *679*, 185–192.

(42) Commoner, B.; Townsend, J.; Pake, G. E. Free Radicals in Biological Materials. *Nature* **1954**, *174*, 689–691.

(43) Chen, C.-T.; Buehler, M. J. Polydopamine and Eumelanin Models in Various Oxidation States. *Phys. Chem. Chem. Phys.* **2018**, *20*, 28135–28143.

(44) Panzella, L.; Leone, L.; Greco, G.; Vitiello, G.; D'Errico, G.; Napolitano, A.; d'Ischia, M. Red Human Hair Pheomelanin Is a Potent Pro-Oxidant Mediating UV-Independent Contributory Mechanisms of Melanomagenesis. *Pigment Cell Melanoma Res.* **2014**, *27*, 244–252.

(45) Solano, F. Melanins: Skin Pigments and Much More—Types, Structural Models, Biological Functions, and Formation Routes. *New J. Sci.* **2014**, *2014*, 1–28.

(46) Sarna, T.; A. Swartz, H. The Physical Properties of Melanins. In *The Pigmentary System: Physiology and Pathophysiology, Second Edition* **2006**, 311–341.

(47) Kim, Y. J.; Khetan, A.; Wu, W.; Chun, S. E.; Viswanathan, V.; Whitacre, J. F.; Bettinger, C. J. Evidence of Porphyrin-Like Structures in Natural Melanin Pigments Using Electrochemical Fingerprinting. *Adv. Mater.* **2016**, *28*, 3173–3180.

(48) Okazaki, M.; Kuwata, K.; Miki, Y.; Shiga, S.; Shiga, T. Electron Spin Relaxation of Synthetic Melanin and Melanin-Containing Human Tissues as Studied by Electron Spin Echo and Electron Sp. *Arch. Biochem. Biophys.* **1985**, 197–205.

(49) Sarna, T.; Hyde, J. S. Electron Spin-Lattice Relaxation Times of Melanin. *J. Chem. Phys.* **1978**, *69*, 1945–1948.

(50) Mostert, A. B.; Hanson, G. R.; Sarna, T.; Gentle, I. R.; Powell, B. J.; Meredith, P. Hydration-Controlled X-Band EPR Spectroscopy: A Tool for Unravelling the Complexities of the Solid-State Free Radical in Eumelanin. *J. Phys. Chem. B* **2013**, *117*, 4965–4972.

(51) Al Khatib, M.; Harir, M.; Costa, J.; Baratto, M.; Schiavo, I.; Trabalzini, L.; Pollini, S.; Rossolini, G.; Basosi, R.; Pogni, R. Spectroscopic Characterization of Natural Melanin from a *Streptomyces Cyaneofuscatus* Strain and Comparison with Melanin Enzymatically Synthesized by Tyrosinase and Laccase. *Molecules* **2018**, *23*, 1916.

(52) Chikvaidze, E. N.; Partskhaladze, T. M.; Gogoladze, T. V. Electron Spin Resonance (ESR/EPR) of Free Radicals Observed in Human Red Hair: A New, Simple Empirical Method of Determination of Pheomelanin/Eumelanin Ratio in Hair. *Magn. Reson. Chem.* **2014**, *52*, 377–382.

(53) Schweiger, A.; Jeschke, G. *Principles of Pulse Electron Paramagnetic Resonance*; Oxford University Press: Oxford, USA, **2001**.

(54) Berliner, L. J.; Eaton, G. R.; Eaton, S. S. *Distance Measurements in Biological Systems by EPR*. Biol. Magn. Reson. **2002**, *19*.

(55) Mihai, I.; Addiégo, F.; Del Frari, D.; Bour, J. Ô.; Ball, V. Associating Oriented Polyaniline and Eumelanin in a Reactive Layer-by-Layer Manner: Composites with High Electrical Conductivity. *Colloids Surfaces A Physicochem. Eng. Asp.* **2013**, *434*, 118–125.

(56) Grossmann, B.; Moll, T.; Palivan, C.; Ivan, S.; Gescheidt, G. Electron Delocalization in One-Electron Oxidized Aniline Oligomers , Paradigms for Polyaniline . A Study by Paramagnetic Resonance in Fluid Solution. *J. Phys. Chem. B* **2004**, *108*, 4669–4672.

(57) Magon, C. J.; De Souza, R. R.; Costa-Filho, A. J.; Vidoto, E. A.; Faria, R. M.; Nascimento, O. R. Spin Dynamics Study in Doped Polyaniline by Continuous Wave and Pulsed Electron Paramagnetic Resonance. *J. Chem. Phys.* **2000**, *112*, 2958–2966.

(58) De Salas, F.; Pardo, I.; Salavagione, H. J.; Aza, P.; Amougi, E.; Vind, J.; Martínez, A. T.; Camarero, S. Advanced Synthesis of Conductive Polyaniline Using Laccase as Biocatalyst. *PLoS One* **2016**, *11*, 1–18.

TOC Graphic